Inverse Identification of the Bond-Slip Law for Sisal Fibers in High-Performance Cementitious Matrices

S. R. Ferreira[1], M. Pepe[2], E. Martinelli[2(✉)], F. A. Silva[3], and R. D. Toledo Filho[1]

[1] Civil Engineering Department, COPPE, Federal University of Rio de Janeiro, Rio de Janeiro, Brazil
[2] Department of Civil Engineering, University of Salerno, Fisciano, Salerno, Italy
e.martinelli@unisa.it
[3] Civil Engineering Department, Pontifical Catholic University of Rio de Janeiro, Rio de Janeiro, Brazil

Abstract. The use of Natural Fibers (NFs) in Fiber-Reinforced Cementitious Composites (FRCCs) is an innovative technical solution, which has been recently employed also in High-Performance FRCCs. However, NFs are generally characterized by complex microstructure and significant heterogeneity, which influence their interaction with cementitious matrices, whose identification requires further advances in the current state of knowledge. This paper presents the results of pull-out tests carried out on sisal fibers embedded in a cementitious mortar. These results are considered for identifying the bond-slip law that describes the interaction between the sisal fibers and the cementitious matrix. A theoretical model, capable of simulating the various stages of a pull-out test, is employed as part of an inverse identification procedure of the bond-slip law. The accuracy of the resulting simulations demonstrates the soundness of the proposed theoretical model for sisal fibers embedded in a cementitious matrix.

Keywords: Sisal fibers · Fiber Reinforced Cementitious Composites
Bond-slip law · Pull-out test · Inverse identification

1 Introduction

In the last decade many researches have been developed with the aim of exploring the potential of composite materials, based on either polymeric or cementitious matrices, internally reinforced by fibers derived by plant leaves or branches (Netravali and Chabba 2003). These fibers, generally referred to as either "vegetal" or "natural", highlighted promising properties in terms of both strength (Silva et al. 2010) and durability (Melo Filho et al. 2013, Ferrara et al. 2014; Ferrara et al. 2015). Moreover, they have an apparent potential for enhanced sustainability with respect to similar materials reinforced with industrial fibers made of either steel (Toledo Filho 1997) or plastic fibers (Sreekumar et al. 2009).

The aforementioned researches unveiled the multifold potential of Natural-Fiber-Reinforced Cementitious Composites in reducing the demand of raw materials, as they are mainly based on using renewable resources, and the supply and production costs, as the original plants are widely available, especially in tropical and sub-tropical zones.

Among the various Natural Fibers (NFs) investigated so far, those made from sisal (*agave sisalana*) leaves (Silva et al. 2009) have attracted a great interest in both material scientists and concrete technologists (Netravali and Chabba 2003). More specifically, their excellent properties in terms of tensile strength is the main motivation for using them as a reinforcement in composite materials (Silva et al. 2008). However, it should be recognized that the weak chemical bonds that can be established with matrices based on Portland cement results in low mechanical bond between these fibers and matrices, whose maximum strength might be estimated in the range of 0.32 and 0.72 MPa, according to experimental results reported in the scientific literature (Silva et al. 2011). Moreover, the high water absorption capacity of sisal fibers results in a volume expansion when they are added to the fresh cementitious matrix and, conversely, it produces a contraction when the matrix dries and, hence, a partial detachment between fibers and matrix at the hardened state.

Different procedures have been proposed for reducing water absorption capacity in natural fibers and improving fiber-matrix bond interaction: they are based on applying chemical and physical treatments of both matrix and fibers (Ferraz et al. 2011). For instance, the partial replacement of cement with *microsilica* have led to increasing the pullout resistance by about 24% (Toledo Filho 1997). This increase is related to the fineness of microsilica, which is capable to reduce porosity in the transition zone, hence enhancing the fiber-matrix bond. Furthermore, the use of alkaline solutions (Saha et al. 2010; Kundu et al. 2012) removes most of the surface non-cellulosic substances and increases roughness of their surface, hence enhancing the fiber-matrix bond. Simple treatments, such as soaking the fibers in distilled water followed by a drying process, also result in improving the fiber-matrix bond (Li et al. 2008). Moreover, a reduction in the fiber hydrophilicity can be achieved by means of wetting and drying cycles promoting *hornification* (namely, stiffening of the polymeric structure present in ligno-cellulosic materials, as defined by Claramunt et al. 2010). This treatment promotes a reduction in volumetric changes of pulps and fibers of natural origin, as well as a significant alteration in their mechanical properties, while acting also as a bridge between fibers and cementitious matrices and, hence, strengthening the interfacial bond (Claramunt et al. 2010).

This paper summarizes the results of pull-out tests carried out on *hornified* sisal fibers embedded in a cementitious mortar. Then, these results are employed in identifying the bond-slip law that describes the interaction between sisal fibers and cement-based matrix: an inverse identification procedure, based on a theoretical model capable of simulating the various stages of a pull-out test, is applied for this task (Ferreira et al. 2016).

2 Experimental Program

2.1 Materials and Processing

The sisal fibers used in the present study were obtained from sisal plants growing in farms located in the Bahia state, Brazil. They were extracted from the sisal plant leaves in the form of long fiber bundles: this process was executed by means of semi-automatic scrapers.

As regards microstructure, it consists of numerous individual fibers (fiber-cells), which are about 6-30 μm in diameter. The individual fiber-cells are linked together by means of the middle lamella. The chemical composition of sisal fibers includes approximately 60.5% cellulose, 25.7% hemicellulose, 12.1% lignin, 1% pectin and 1.6% ash (Fidelis 2012; Silva et al. 2009; Silva et al. 2010).

The cement-based matrix presented a mix design of 1:0.5:0.4 (binder: sand: water/binder ratio) by weight.

The binder was composed by 30% of Portland cement CP-32 F II, 30% of meta-kaolin and 40% of fly ash. This ratio of metakaolin and fly ash was aimed to guarantee the durability of the fiber once a matrix free of calcium hydroxide is obtained (Toledo Filho et al. 2009; Melo Filho et al. 2013).

The fly ash also ensured higher workability to the matrix that, within the context of high-performance composites, is a desirable property, as it provided a better homogenization of the natural fibers (Ferreira et al. 2015).

The sand was processed to obtain a maximum diameter of 840 μm and the superplasticizer was the Glenium 51 (type PA) with solids content of 31%. In addition, a viscosity modifier Rheomac UW 410, (manufactured by BASF), at a dosage of 0.8 kg/m^3 was also used in order to avoid segregation and bleeding during molding.

The matrix showed a flow table spread value of 450 mm according to the Brazilian standard NBR 13276 (2005) and a compressive strength at 28 days of 31 MPa, according to NBR 7215 (1996).

The mixtures were produced in a room with controlled temperature (21 ± 1 °C) using a mixer with capacity of 5 l. The mixing procedure consisted of the following stages:

– all dry components were homogenized in the mixer;
– the water and superplasticizer were added and mixed for 2 min at a speed of 125 RPM;
– the process was stopped during 30 s to remove the material retained in the mixer;
– the mixing procedure continued for 2 min at 220 RPM and, finally, for a further 5 min at 450 RPM.

A special mold was developed for preparing the specimens. After filling the mold with the matrix, the top cap was fixed and the fiber stretched slightly for alignment. The mortar was placed in plastic bags before being placed in the mold as to facilitate the casting process. Embedment length of 25 was analyzed. After 24 h, the specimens were demolded and placed in a fog room (HR% ≥ 95%) to moist curing for 7 days for the pullout test.

2.2   Hornification Process

The sisal fibers were placed in a container with water (T = 22 °C) during three hours to reach its maximum water absorption capacity. The drying process was carried out in a furnace at a temperature of 80 °C. The furnace used was equipped with an electronic temperature control and connected to a scale, with a tolerance of 0.01 g to record the loss of water.

The furnace was programmed to reach 80 °C at a heating rate of 1 °C/min and to maintain this temperature for 16 h. After 16 h of drying, the furnace was cooled down to the temperature of 22 °C in order to avoid possible thermal shock to the fibers. This procedure was repeated ten times. More details can be obtained elsewhere (Ferreira et al. 2015).

2.3   Testing

The sisal fiber's microstructure was investigated using a Hitachi TM3000 Scanning Electron Microscope (SEM). The microscope was operated under an accelerating voltage of 15 kV. A pre-coating with a thin layer of approximately 20 nm of gold was done to make the fiber conductive and suitable for analysis. In order to measure the fiber's cross-sectional area, for each single fiber used in the pullout and tensile test, an adjacent piece of the fiber (immediately next to the one tested) was kept for future measurement and morphology characterization using the SEM. Fiber-matrix interface zone was also investigated. The obtained images were post-processed using ImageJ, a Java-based image processing program.

The tensile tests were performed in an electromechanical testing machine Shimadzu AG-X with a load cell of 1 kN. The tests were performed on 15 sisal fibers using a displacement rate of 0.1 mm/min. The fibers with a gage length of 50 mm were glued to a paper template for better alignment in the machine and for a better griping with the upper and lower jaws in accordance with ASTM C1557 (2013). To calculate the tensile strength of the fibers, their diameters were measured by image analysis from micrographs obtained in a scanning electron microscope.

The pullout tests were performed in an electromechanical testing machine Shimadzu AG-X with a load cell of 1 kN. The tests were carried out using a displacement rate of 0.1 mm/min. The samples were fixed in the machine grips through a system with hinged-fixed boundary conditions. Fifteen tests were performed (embedded length of 25 mm).

3   Anlytical Modeling

An analytical model has been formulated for simulating the interaction between fiber and matrix in a pull-out process (Ferreira et al. 2016).

It assumes that:

– the fiber behaves in a linear elastic way;
– the matrix is supposed to be perfectly stiff;

– the interaction between fiber and matrix is based on a bond-slip law τ-s, invariant throughout the fiber length.

As for the last point, the model assumes the following bilinear bond-slip law (Fig. 1):

$$\tau(s) = \begin{cases} k_{el} \cdot s & if & |s| \leq s_{el} \\ \tau_r - k_{in} \cdot (s - s_{el}) & if & s_{el} < |s| \leq s_u \\ 0 & if & |s| > s_u \end{cases} \tag{1}$$

where $k_{el} = \tau_{max}/s_{el}$ is the slip modulus of the elastic branch ending at a slip value s_{el} with a corresponding bond stress τ_{max}. Moreover, τ_r is the residual bond stress, and k_{in} is the post-peak slip modulus, strictly positive in Eq. (1), resulting in a linear variation of stresses from τ_r to τ_u, the latter being achieved for a slip s_u.
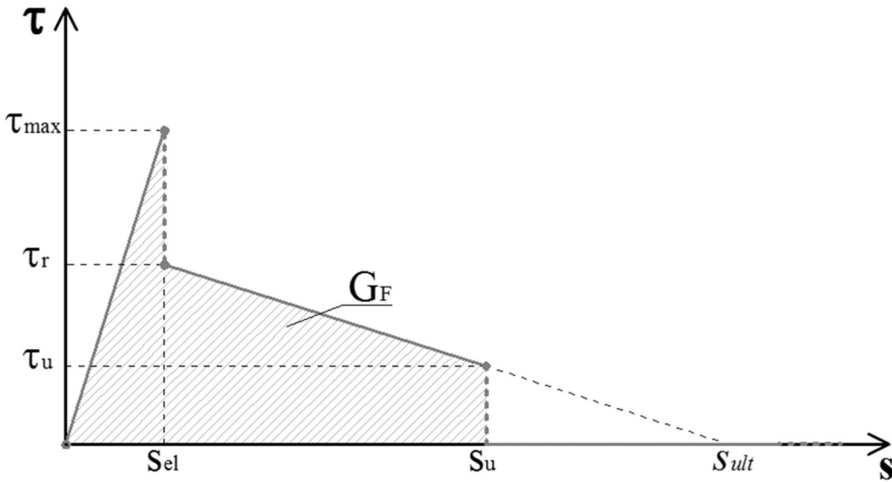

Fig. 1. Bilinear bond-slip law

The equilibrium equation of an infinitesimal element of fiber can be easily determined as already presented in several models already available in the literature (Caggiano et al. 2012), a general equilibrium condition can be determined (Fig. 2):

$$\frac{d\sigma f}{dz} - \frac{P_f}{A_f} \cdot \tau = 0 \tag{2}$$

Moreover, the axial strain ε_f developing in the fiber is strictly related to the interface slip s:

$$\varepsilon_f = \frac{ds}{dz} \tag{3}$$

Since the fiber is elastic $\sigma_f = E_f \epsilon_f$ and, hence, Eq. (3) can be introduced in Eq. (2), in order to obtain a well-known differential relationship between the second derivative of the interface slips and the corresponding bond stress τ (Caggiano et al. 2012):

$$\frac{d^2 s}{dz^2} - \frac{P_f}{E_f A_f} \cdot \tau(s) = 0 \qquad (4)$$
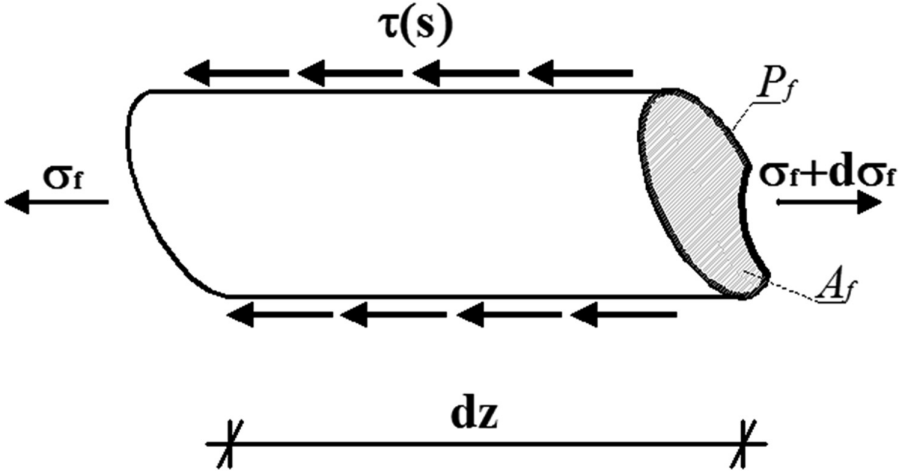

Fig. 2. Local equilibrium conditions on a free infinitesimal element of fiber.

A step-wise analytical solution can be obtained by considering the various states of stresses of the fiber-to-matrix interface resulting from the bilinear bond-slip law represented in Fig. 1. Further details on both the mathematical derivation and the numerical implementation of this solution are available in Ferreira et al. (2016).

Based on the above assumptions, the full range analytical expression of the applied pull-out force F_0 can be, as a function of the displacement s_0 at the end of the fiber embedment, on the loaded side.

Moreover, F_0 also depends upon the actual bond-slip law assumed for describing the interface behavior. Hence, the following conceptual relationship can be written:

$$F_0 = F_0(s_0; \boldsymbol{q}) \qquad (5)$$

where q is a vector that collects the five parameters describing the interface law de-scribed in Fig. 1:

$$\boldsymbol{q} = \begin{bmatrix} s_{el} & s_u & \tau_{max} & \tau_r & \tau_u \end{bmatrix} \qquad (6)$$

The aforementioned analytical model can be employed for determining the parameters describing the actual bond-slip interaction by means of an "inverse identification" procedure (Martinelli et al. 2012). More specifically, the following optimization problem has to be solved:

$$\overline{q} = \underset{q}{arg\,min}\,\Delta(q) \tag{7}$$

being

$$\Delta(q) = \sum_{i=1}^{n} \left[F_0(s_{0,i}; q) - F_{0,i}^{exp} \right]^2 \tag{8}$$

where $s_{0,i}$ is the displacement imposed on the free end of the fiber at the i-th increment of the experimental procedure, $F_{0,iexp}$ is the corresponding force and n is the number of displacement increments either in the experimental process or the current numerical analysis.

4 Results and Analysis

4.1 Morphological Characterization of Sisal Fiber

Table 1 summarizes the results derived from the SEM analysis by presenting the measured value in terms of area, perimeter and fiber's shape.

Table 1. Sisal fibers geometry

#	Area mm^2	Perimeter mm	Shape
1	0.01478	0.7900	Twisted
2	0.01739	0.8200	Twisted
3	0.03750	1.2300	Twisted
4	0.01753	0.6114	Horse shoe
5	0.01115	0.5619	Twisted
6	0.02270	0.8739	Twisted
7	0.01650	0.5330	Horse shoe
8	0.01641	1.0300	Twisted
9	0.02970	0.8281	Horse shoe
10	0.01571	0.5683	Arch
11	0.02391	1.0600	Twisted
mean	0.02030	0.8097	–

Based on the values of parameters reported in Table 1, the hornified sisal fiber presents high scattering in terms of morphological characterization. The area and perimeter values range from 0.001 to 0.003 mm^2 and 0.53 to 1.3 mm, respectively. This significant variation might be directly related to the significant variability in the shape of fibers' cross-sections.

This clue is confirmed by Fig. 3, which shows the three typical cross-section shapes exhibited by sisal fibers, each one presenting a different relationship between cross-section area and perimeter.
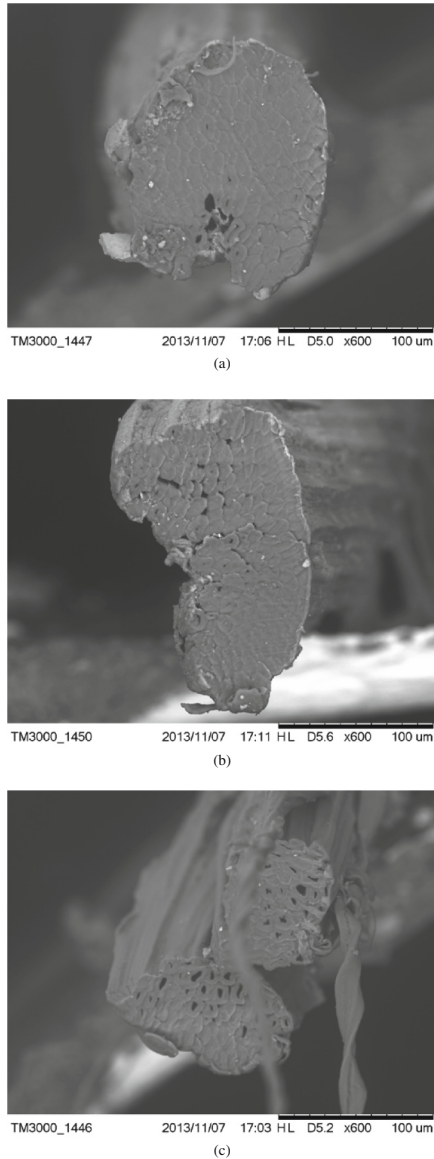
Fig. 3. Sisal fiber shape: horse shoe (a), arch (b), twisted (c).

As a matter of fact, within the leaf, there are three basic types of fibers, generally referred to as structural, arch and xylem fibers (Silva et al. 2011). Structural fibers have a *horse shoe* shape and a rough surface (Fig. 3a); *arch* shape fibers (Fig. 3b) grow in association with the conducting tissues of the plant (usually found in the middle of the leaf); *xylem* fibers grow opposite to the arch fibers, presenting a *twisted* shape (Fig. 3c), similar to double-helical DNA model.

4.2   Mechanical Properties

The results in terms of tensile strength and the corresponding elastic modulus for both untreated and hornified sisal fibers are summarized in Table 2. They show that hornification induce to a slight increase in tensile strength and strain at failure (about 5%), while it reduces the elastic modulus.

Table 2. Tensile tests results.

Treatment	Tensile strength		Elastic modulus	
	MPa	CoV (%)	GPa	CoV (%)
Natural	453.23	66.49	20.16	3.52
Hornification	474.86	26.46	18.05	2.75

In fact, wetting and drying cycles change the microstructure in natural fibers, which, in turn, modifies the polymeric structure of the fiber-cells resulting in higher tensile strength and strain. Moreover, it is worth highlighting that hornification reduces the variability affecting the mechanical response of sisal fibers, both in terms of tensile strength (coefficient of variation slumps from 67 to 26%) and elastic modulus (CoV reduces from 3.5 to 2.7%).

4.3   Bond-Slip Law Identification

The results of the inverse identification of the bond-slip laws performed on hornified sisal single fiber pull-out tests, are summarized in Table 3.

A total number of 15 tests were performed (embedded length equal to 25 mm), but 4 samples exhibited fiber fracture and for this reason their results are not considered in the present analysis for the bond-slip law identification.

Table 3. Parameters of the identified bond-slip law results.

#	s_e	s_u	τ_{max}	τ_r	τ_u	G_F
	mm	Mm	MPa	MPa	MPa	Nmm
1	0.08	2.96	0.31	0.28	0.21	0.36
2	0.11	4.19	0.27	0.22	0.13	0.36
3	0.50	8.05	0.14	0.13	0.09	0.41
4	0.28	5.22	0.35	0.27	0.25	0.86
5	0.30	5.21	0.44	0.30	0.29	1.12
6	1.57	5.76	0.27	0.13	0.02	0.53
7	1.31	5.20	0.62	0.34	0.13	1.20
8	0.20	7.90	0.39	0.19	0.15	1.40
9	1.00	5.55	0.15	0.12	0.08	0.30
10	0.36	3.35	0.31	0.26	0.12	0.31
11	0.62	3.95	0.20	0.20	0.19	0.38
mean	0.58	5.21	0.31	0.22	0.15	0.66
CoV (%)	86.7	31.5	44.5	34.0	52.4	62.1

The quality of the approximation that can be achieved by means of the proposed model is demonstrated by comparing experimental results and analytical simulations (in terms of F_0-s_0 curves) for each test (Fig. 4). The curves clearly demonstrate that the analytical solution proposed in this study is capable of accurately reproducing the bond behavior of hornified sisal fibers embedded in a cement matrix.

However, the results reported in Table 3 highlight that the bond-slip laws identified for the various tests are fairly scattered. In other words, defining a unique bond-slip law capable to describe the bond behavior of natural fibers in cement matrix does not seem realistic. This can be justified by considering that sisal fibers are heterogeneous, in terms of both mechanical and geometric properties, and this heterogeneity leads to a significant variability in the resulting adhesion with mortar. In fact, the resulting bond behavior in cement matrix is influenced by several parameters, such as fiber shape, fiber cross section area variation along the longitudinal axis and surface texture and roughness of the filaments.

Nevertheless, the identified bond-slip laws may be analyzed and compared in terms of some key mechanical parameters, such as the specific fracture energy G_F, which represents the area under the local bond-slip law in Fig. 1.

Before commenting into details the results in Table 3, it should be mentioned that the bond behavior of fibers in cement matrix can be mainly divided in three phases: adhesion, mechanical bond and frictional bond (Naaman, 1999). The first two mainly depends on the chemical compatibility between the fiber and the matrix and the surface texture of the fiber while the latter is, mainly, governed by the geometrical characteristic of the fiber.

Then, the values of G_F reported in Table 3 can be interpreted in the light of the above considerations.

As regards fracture energy, it should be noticed that the high dispersion, in terms of coefficient of variation CoV (around 60% as highlighted in Table 3), presented by the G_F can be mainly attributed to the morphological characteristics of sisal fibers. In fact, these fibers are characterized by a high variability in terms of transverse section properties (P_f and A_f) as well as in terms of overall straightness and this heterogeneity
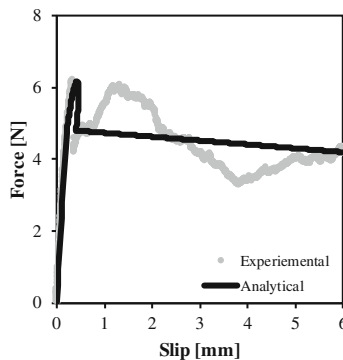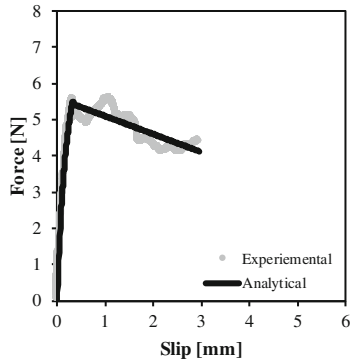

(a)

Fig. 4. Simulation examples of the force-slip response
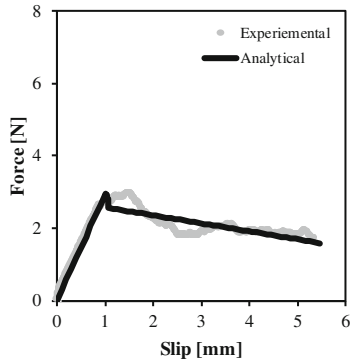
(b)

(c)

Fig. 4. (*continued*)

influence the frictional bond mechanisms that play a fundamental role on the definition of the fracture energy.

Conversely, the values of τ_{max} presents a lower value in terms of CoV. This can be explained by considering that the elastic branch is mainly controlled by the adhesion and mechanical bond mechanism occurring between fiber and matrix, both being more related to the chemical adhesion between sisal fiber and cement based matrix, rather than their geometric properties.

5   Conclusions

This paper was intended at investigating the bond behavior of hornified sisal fibers embedded in cement-based matrix. On the one hand, the reported experimental results demonstrate the potential of using sisal fibers as spear reinforcement in cementitious composites. On the other hand, the proposed theoretical model leads to scrutinizing the local bond-slip relationship characterizing the interaction between fiber and matrix.

The following main points can be remarked:

– the pull-out tests highlighted good bond properties of hornified sisal fibers: since the majority of specimens failed in debonding, one can reasonably recognize that their transfer length is longer than 25 mm and, hence, the majority of the tested specimens can be considered for charactering the bond behavior of sisal fibers;
– an analytical model, already formulated by the Authors for similar problems, was extended to the case of hornified fibers by introducing a more general bi-linear bond-slip law, whose characteristic features (e.g. discontinuities and non-zero ultimate stresses) resulted essential in simulating the observed behavior of the fibers under consideration;
– in spite of the significant variability affecting the geometry of fibers, reasonably stable values of the key parameters of the identified bond-slip laws were determined for the various tested specimens. Particularly, the variability of two main parameters, such as bond strength and fracture energy was analyzed.

The results of this study will pave the way towards a comprehensive understanding of the mechanical behavior of cementitious composites reinforced by natural fibers. Particularly, the research will move toward the structural scale by analyzing the response of structural members made of this the materials considered herein. Moreover, the proposed analytical model will be available for identifying the bond-slip laws resulting for other kinds of natural fibers (i.e. jute and curauá) and compare them with the one determined for hornified fibers.

References

ASTM standard C1557 (2013) Standard test method for tensile strength and young's modulus of fibers, ASTM International, West Conshohocken, PA

Caggiano A, Martinelli E, Faella C (2012) A fully-analytical approach for modelling the response of FRP plates bonded to a brittle substrate. Int J Solids Struct 49(17):2291–2300

Claramunt J, Ardanuy M, Garcia-Hortal JA (2010) Effect of drying and rewetting cycles on the structure and physicochemical characteristics of softwood fibres for reinforcement of cementitious composites. Carbohydr Polym 79:200–205

Ferraz JM, Menezzi CHS, Texeira DE, Martins SA (2011) Effects of treatment of coir fiber and cement/fiber ration on properties of cement-bonded composites. BioResources 3:3481–3492

Ferrara L, Ferreira SR, Krelani V, Silva F, Toledo Filho RD (2014) Effect of natural fibres on the self healing capacity of high performance fibre reinforced cementitious composites. In: Proceedings SHCC3, 3rd international RILEM conference on strain hardening cementitious composites, pp 9–16

Ferrara L, Ferreira SR, Krelani V, della Torre M, Silva F, Toledo Filho RD (2015) Natural fibres as promoters of autogeneous healing in HPFRCCS: results from on-going brazil-italy cooperation, special publication, vol. 305, pp 11.1–11.10

Ferreira SR, de Andrade Silva F, Lima PRL, Toledo Filho RD (2015) Effect of fiber treatments on the sisal fiber properties and fiber–matrix bond in cement based systems. Constr Build Mater 101:730–740

Ferreira SR, Martinelli E, Pepe M, de Andrade Silva F, Toledo Filho RD (2016) Inverse identification of the bond behavior for jute fibers in cementitious matrix. Compos Part B Eng 95:440–452

Fidelis MEA (2012) Development and mechanical characterization of jute textile reinforced concrete (Doctoral Thesis), Civil Engineering Department, Universidade Federal do Rio de Janeiro (COPPE/UFRJ). (in Portuguese)

Kundu SP, Chakraborty S, Roy A, Adhikari B, Majumber SB (2012) Chemically modified jute fibre reinforced non-pressure (NP) concrete pipes with improved mechanical properties. Construct Build Mater 37:841–850

Li Y, Hu C, Yu Y (2008) Interfacial studies of sisal fiber reinforced high density polyethylene (HDPE) composites. Compos Part A Appl Sci Manuf 4:570–578

Martinelli E, Napoli A, Nunziata B, Realfonzo R (2012) Inverse identification of a bearing-stress-interface-slip relationship in mechanically fastened FRP laminates. Compos Struct 94(8):2548–2560

Melo Filho JA, Silva FA, Toledo Filho RD (2013) Degradation kinetics and aging mechanisms on sisal fiber cement composite systems. Cem Concr Compos 40:30–39

Naaman AE (1999) Fibers with slip-hardening bond. In: PRO 6: 3rd international RILEM workshop on high performance fiber reinforced cement composites (HPFRCC 3), pp 371–385

NBR 13276 (2005) Mortars applied on walls and ceilings - preparation of mortar for unit masonry and rendering with standard consistence index. ABNT, Rio de Janeiro

NBR 7215 (1996) Portland cement - determination of compressive strength, ABNT, Rio de Janeiro

Netravali AN, Chabba S (2003) Composites get greener. Mater Today 6:22–29

Saha P, Manna S, Chowdhury SR, Sen R, Roy D, Adhikari B (2010) Enhancement of tensile strength of lignocellulosic jute fibres by alkali-steam treatment. Bioresour Technol 101:3182–3187

Silva FA, Chawla N, Toledo Filho RD (2008) Tensile behavior of high performance natural (sisal) fibers. Compos Sci Technol 68:3438–3443

Silva FA, Mobasher B, Soranakom C, Toledo Filho RD (2011) Effect of fiber shape and morphology on interfacial bond and cracking behaviors of sisal fiber cement based composites. Cem Concr Compos 33:814–823

Silva FA, Mobasher B, Toledo Filho RD (2009) Cracking mechanisms in durable sisal reinforced cement composites. Cem Concr Compos 31:721–730

Silva FA, Toledo Filho RD, Melo Filho FA, Fairbairn EMR (2010) Physical and mechanical properties of durable sisal fiber cement composites. Construct. Build. Mater 24:777–785

Sreekumar PA, Thomas SP, Saiter JM, Joseph K, Unnikrishnan G, Sabu T (2009) Effect of fiber surface modification on the mechanical and water absorption characteristics of sisal/polyester composites fabricated by resin transfer molding. Compos Part A Appl Sci Manuf 40:1777–1784

Toledo Filho RD (1997) Materiais compósitos reforçados com fibras naturais: caracterização experimental. Doctoral thesis, Civil Enginnering Department, PUC-Rio, Rio de Janeiro, Brazil. (in portuguese)

Toledo Filho RD, Silva FA, Melho Filho JA, Fairbairn EMR (2009) Durability of compression molded sisal fiber reinforced mortar laminates. Construct Build Mater 23:2409–2420